



ASRT



Bulletin of Faculty of Science - Zagazig University

<https://bfszu.journals.ekb.eg>



FS-ZU

Investigate Structural and electrical properties of PVA/ α - Al_2O_3 /P(GO)composites

A. F. Mansour¹, S. F. Mansour^{1,2}, M. A. Abdo^{1,*}, R. M. Dahshan¹

¹Physics Department, Faculty of Science, Zagazig University, Zagazig, Egypt

²Physics Department, Faculty of Science, King Abdulaziz University, Jeddah, Saudia Arabia

ARTICLE HISTORY

Received: June/2018

Revised: July/2018

Accepted: November/2018

KEY WORDS

PVA

α - Al_2O_3 nanoparticles

P(GO)

nano composite

ABSTRACT: In the sitting study, Partially- reduced graphene oxide P(GO) was prepared from the graphite powder according to the modified Hummers d PVA / α - Al_2O_3 / P(GO) were prepared by casting method with compositions (w/w between P(GO) and PVA α - Al_2O_3 /: 0%, 0.3%, 0.9% and 1.5%). The samples were recognized by X-ray diffraction (XRD), FTIR analysis and the electric properties were studied. The XRD pattern and FTIR analysis showed that the as prepared P(GO)is in pure single phase. The XRD patterns and FTIR analysis of P(GO)/ PVA/ Al_2O_3 composites confirmed the formation of P(GO)/ PVA\ α - Al_2O_3 composite films without any impurities. FTIR analysis of P(GO)/ PVA composites confirmed the presence of the two phases without any other phase. The temperature dependence of dielectric constant (ϵ') as a function of frequencies for P(GO)/ PVA/ α - Al_2O_3 composites was measured and indicated that the dielectric constant decrease with increasing frequency and increase gradually with increasing temperature. The temperature dependence of ac. electrical conductivity as a function of frequencies for P(GO)/ PVA/ α - Al_2O_3 composites was determined. The results showed that presence of two different conduction mechanisms.

*Corresponding Author: mhmd_ahmd20@yahoo.com

1. INTRODUCTION

Nanoparticles research is presently an objective domain of scientific weal due to its potential applications in several fields from optical, electrical to biological. Metal oxide nanoparticles have been exceedingly improved

in the past decennium. They have been vastly utilized in numerous applications such as catalysts, sensors, semiconductors, medical science, capacitors, and batteries (Ueda et al,2008,Gessner et al,2000, Kim et al,2005, Pria,

2007, Farsi and Gobal,2007,Dillon et al,2008). Amid them, aluminum oxide, Al_2O_3 , is transpiring. Alumina has sundry phases such as gamma, delta, theta, and alpha, the far the st thermodynamically stable form is $\alpha\text{-Al}_2\text{O}_3$ (Mallakpour1,2 and Dinari,2013). Al_2O_3 has become more prevalent for their high dielectric strength, a wide optical band gap, exceptional stability, and durability against hostile environments and high transparency down to 250 nm. Also, $\alpha\text{-Al}_2\text{O}_3$ has been excessively utilized for their practical applications, such as refractory coatings, antireflection coatings, anticorrosive coatings (Dillon et al,2008), microelectronic devices (Chang et al,1989), capacitance humidity sensors (Nahar,1982), and silicon solar cells (Werner et al,2012), and as insulating material, in the form of thin films, in semiconductor devices (Boratto et al,2014). Polymer nanocomposites have been elaborated for their marvelous properties such as light weight, high flexibility, and ability to be feigned at low temperature and low cost, and application in various fields such as radiation detection, coating, paints, sensors, LEDs, display, optoelectronics devices and biological application (Thomas,2010,Mai et al,2006,Sahi,2016,Tantis and Psarras,2012). Graphene is a two-dimensional (2D) material that has attracted significant interest in the scientific community due to its interesting electronic, optical, and thermal properties. The high carrier mobility of graphene and large maximum current density make it a promising candidate for post silicon electronics (Morozov et al,2008) Water soluble graphene oxide (GO) can be used as the additives of other materials to change their structure or properties (Ghosh et al,2016,Liu et al,2017,Xiang et al,2018,Dervin,2017,Ren,2018). The main goal of this work is to investigate the polymer nanocomposites, PVA/ $\alpha\text{-Al}_2\text{O}_3$ and PVA / $\alpha\text{Al}_2\text{O}_3$ /P(GO) and then compare between the optical properties of them.

2. EXPERIMENTAL

Partially- reduced graphene oxide P(GO) was prepared from the graphite powder

according to the modified Hummers and Offman method (Hummers and Offeman,1958). Extra pure graphite powder (2.0 g, 12.0 g/ mole, 99.5%) was pre-oxidized by slowly adding it to a solution of concentrated sulfuric acid (H_2SO_4 , 50 ml, Dongwoo fin chem, 95- 97%) and concentrated nitric acid (HNO_3 , 50 ml, Dongwoo fin chem, 68- 70%) followed by stirring at 80oC for 4 hours. The mixture was cooled down to room temperature and then washed by de-ionized water until the PH value was neutral (equal to 7.0), followed by drying at 40 °C overnight. The resultant pre-oxidized graphite was dispersed into concentrated H_2SO_4 in a cold reaction vessel, which was kept in an ice bath and stirred, followed by slow addition of potassium permanganate (KMnO_4 , 10 g, Sigma Aldrich, 97%). The temperature was held below 10°C during the addition. The mixture was stirred at 35°C for 2 hours, during which time the solution thickened and turned into a brownish gray in color. Then 250 ml of de-ionized water was added and the temperature was raised to 100°C for 15 minute. Then 700 ml of de-ionized water and 30 ml hydrogen peroxide (H_2O_2 , Dongwoo fin chem, 30%) were added and followed by stirring for 1 hour. The solid products collected from the solution after 12 hours, then washed with 5% hydrochloride (HCl) until sulphate ions were no longer detectable with barium chloride (BaCl_2). Then the solid products were re-dispersed in de-ionized water for 5 times to remove any impurities. Finally the resultant sediment was dried at 60°C for 4 hours in an oven to yield the partially reduced graphene oxide P(GO).By chosen the nanocomposite with 5% from $\alpha\text{-Al}_2\text{O}_3$ / PVA the composite films of PVA/ $\alpha\text{Al}_2\text{O}_3$ /P(GO) were prepared by casting method with composition 0.0015, 0.0045,and 0.0075, gm of PGO. The mixture is put in a petri dish and leave to dry. The X-ray diffraction (XRD) patterns were recorded at room temperature using an X-ray powder diffractometer (Shimadzu XRD 6000) equipped with CuK_α as radiation source ($\lambda = 1.54\text{\AA}$.) in the 2θ (Bragg angles) range ($10^\circ \leq 2\theta \leq 80^\circ$) to report the information about their structure.

3. RESULTS AND DISCUSSION

3.1. Structural properties

The X-ray diffraction (XRD) is the most common analysis technique used to identify the crystalline phase present and crystal particle sizes.

The X-ray diffraction pattern for partially-reduced graphene oxide P(GO) sample is shown in Fig.(1). The XRD pattern showed a sharp diffraction peak located at $2\theta = 10.53^\circ$ and a small peak located at $2\theta = 42.39^\circ$ which corresponding to (001) and (100) reflection plane of GO (Huanget al,2012,Balasu et al ,2013,Shahriary and Anjali,2014). Furthermore, a broad peak located around $2\theta = 32^\circ$ (inset curve) is attributed to reduced graphene oxide R(GO) obtained by Wu et al.(Wu et al,2012)and Zhang et al.(Zhang et al,2013). Finally, we conclude that, our prepared sample is partially-reduced graphene oxide P(GO).

The X-ray diffraction patterns for P(GO)/PVA/ α - Al_2O_3 composite films are shown in Fig. (2). XRD patterns of all P(GO)/PVA/ α - Al_2O_3 films showed a broad peak at $2\theta = 19.74^\circ$, which is attributed to the polyvinyl alcohol (PVA). The diffraction peak which is attributed to P(GO) not observed, because the concentration of P(GO) is very low compared with that of PVA. Also the observed peaks at $2\theta = 35.11^\circ, 43.33^\circ, 52.51^\circ, 57.45^\circ, 66.53^\circ$ and 68.23° , which is attributed to the alumina (α -

Al_2O_3). These diffraction peaks confirmed the formation of P(GO)/PVA/ α - Al_2O_3 composite films without any impurities. XRD patterns of

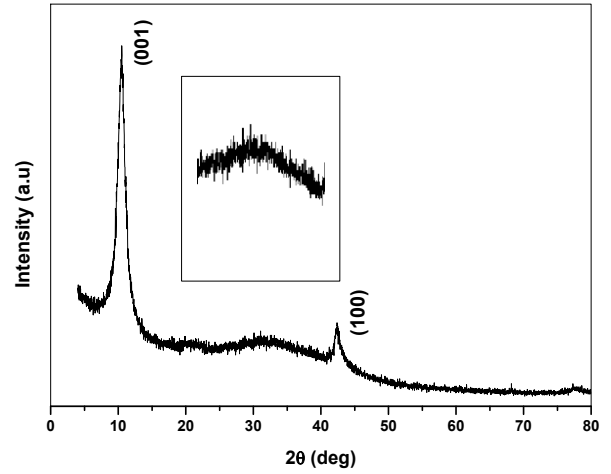


Fig. 1: XRD pattern of P(GO).

pure PVA, pure P(GO) and its composites indicating that there is no interaction between polyvinyl alcohol and the partially-reduced graphene oxide in forming composites.

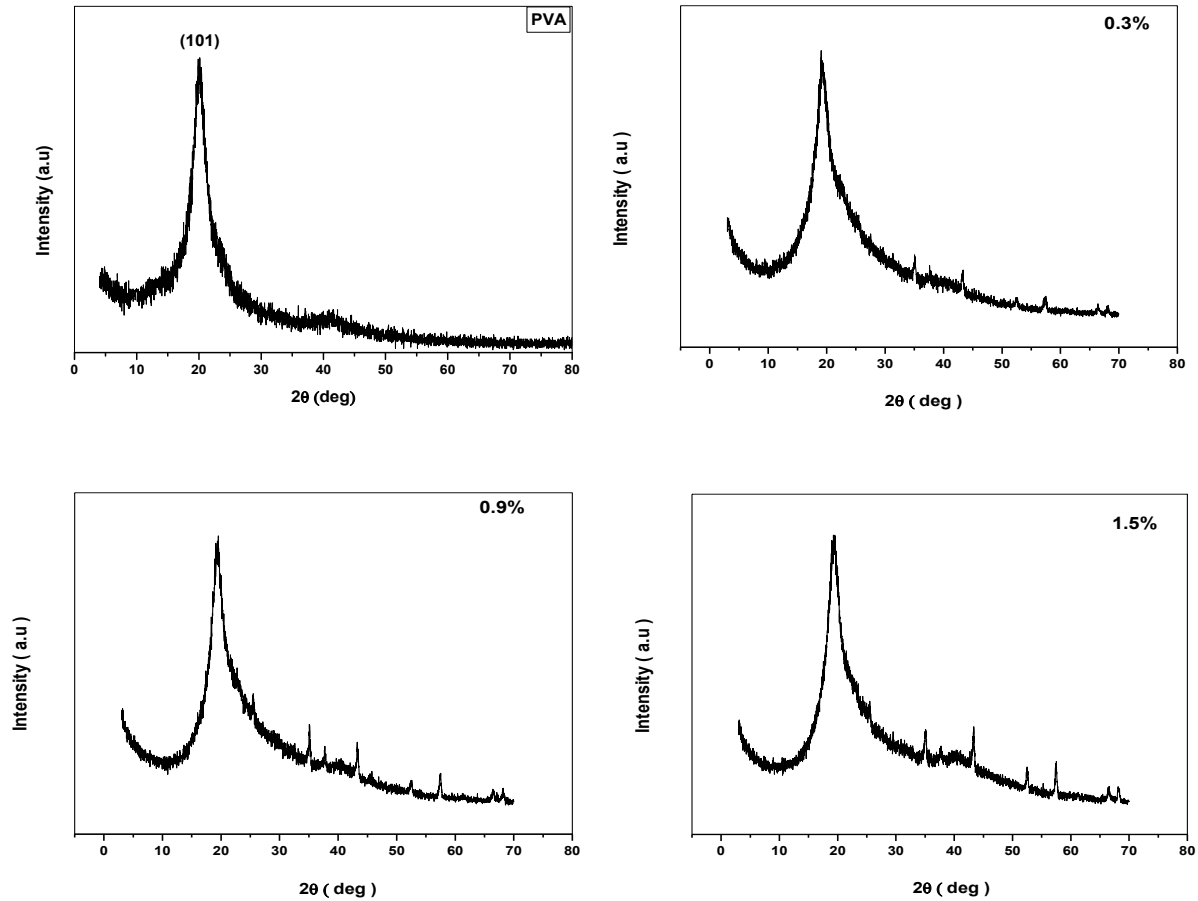


Fig. 2: XRD pattern of: pure PVA and P(GO)/ PVA/ α -AL₂O₃ composite films.

3.2. FTIR analysis:

The FTIR spectra for pure P(GO) is shown in Fig. 3. The broad band centered at 3440 cm^{-1} is attributed to the stretching vibration of hydroxyl group (OH). The band observed at 1625 cm^{-1} is attributed to the non-oxidized graphite (Si and Samulski, 2008). The band observed at 1380 cm^{-1} is assigned to the symmetric stretching vibrational band of C=O (Jothi Ramalingam et al., 2014). Furthermore, the band observed at 1050 cm^{-1} is attributed to the stretching vibrational band of C-O (Xu et al., 2008). Finally, the two bands observed at 2920 and 2855 cm^{-1} are assigned to stretching vibrational band of C-H, which is characterized the FTIR spectrum of reduced graphene oxide

obtained by Chen et al. (Chenet al, 2012) and Zhang et al. (Zhang et al, 2014). Thus, we conclude that, our sample is partially-reduced

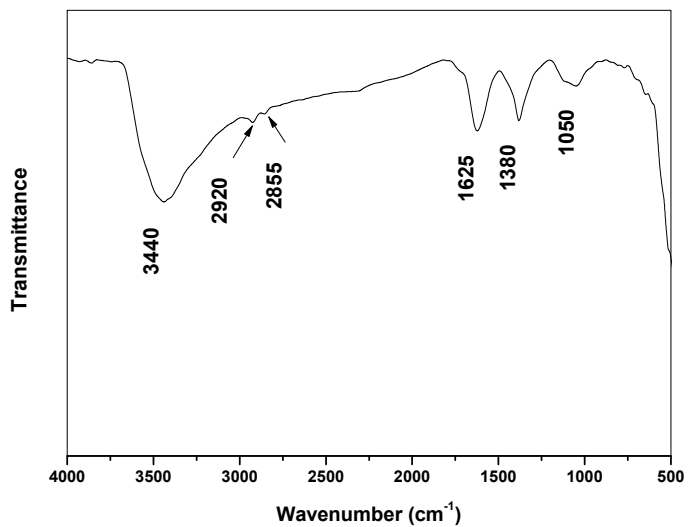


Fig. 3: FTIR spectrum of P(GO).

graphene oxide.

In the spectra of P(GO)/ PVA/ α -Al₂O₃ composites, see Fig. 4, the broad and strong band centered at 3340 cm⁻¹ is assigned to the stretching vibration of hydroxyl group (OH) (Yuan,2011). The strong band at 2940 cm⁻¹ is assigned to the band of asymmetric CH₂ stretching (Roy et al, 2013). The two bands observed at 1712 and 1658 cm⁻¹ are assigned to the stretching vibrational band of C=O (Gunassekaran et al, 2009). The two bands observed at 1427 and 1330 cm⁻¹ are assigned as CH₃ bending vibration and CH₂ stretching respectively (Keskin et al, 2011). The band at 1090 cm⁻¹ arises from the C–O stretching vibration while the band at 920 cm⁻¹ results from CH₂ rocking vibration (Ali and Youssef, 2007). Also, the band at 850 cm⁻¹ results from

C–C stretching vibration and that at 660 cm⁻¹ arises from out of plane OH bending (Hemalatha et al,2014). The absorption bands in the range of 600–400 cm⁻¹ are attributed to the Al–O stretching FTIR spectra of PVA, P(GO) and its composites indicating that there are no interactions between polyvinyl alcohol and partially- reduced graphene oxide in forming composites.

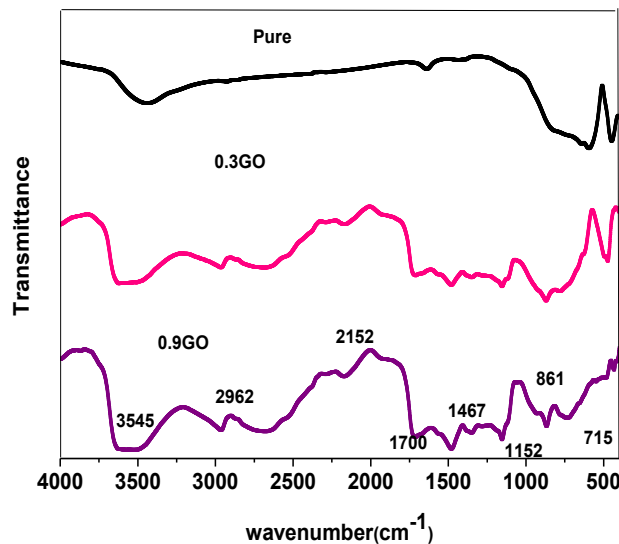


Fig. 4: FTIR spectra of P(GO)/ PVA/ α -AL₂O₃ composite films, and pure α -AL₂O₃

3.3. Electrical properties

Fig. 5 correlates the variation of the dielectric constant ϵ' with the absolute temperature in the frequency range 10 kHz –5 MHz for 5% α -Al₂O₃/ PVA and PVA/ α -Al₂O₃/P(GO) composite films. At initial temperature (30°C) these plots do not show any change in ϵ' value which shows that there is no accumulation of interfacial charge within the composites. As the temperature gradually increased, it was observed that dielectric constant also increased and at 150°C, ϵ' value for the sample having higher percent of nano

alumina was maximum. The increase in dielectric constant can be attributed to the fact that near the glass transition temperature, segmental mobility of the polymer chains gave high rise in dielectric constant for all the samples. Thus dielectric property provided valuable information such as characteristic of the ionic/molecular interaction of the polymer and the understanding of ion transport behavior as well. Furthermore, the increase in dielectric constant indicates the increase of the number of ions and ϵ' (Ng et al,2011). Also, the decrease in ϵ' with increasing frequency is due to the fast alternation of the electric field accompanied with the applied frequency, where the alternation of the ions increases as well as the

friction between them, generating a quantity of heat which increases the randomness of the ions. In other words at low frequency the mobile ions accumulate at the electrode/ composite interface (space-charge polarization). This gives a high value of dielectric constant. On the other

surface electric charges and the concentration 0.3% wt has the highest one. Fig. (6) show the relation between $\ln\sigma_{ac}$ (σ_{ac} is the alternating current conductivity) and the reciprocal of absolute temperature for P(GO)/ PVA/ α - Al_2O_3 composites in the frequency range 10 kHz- 5

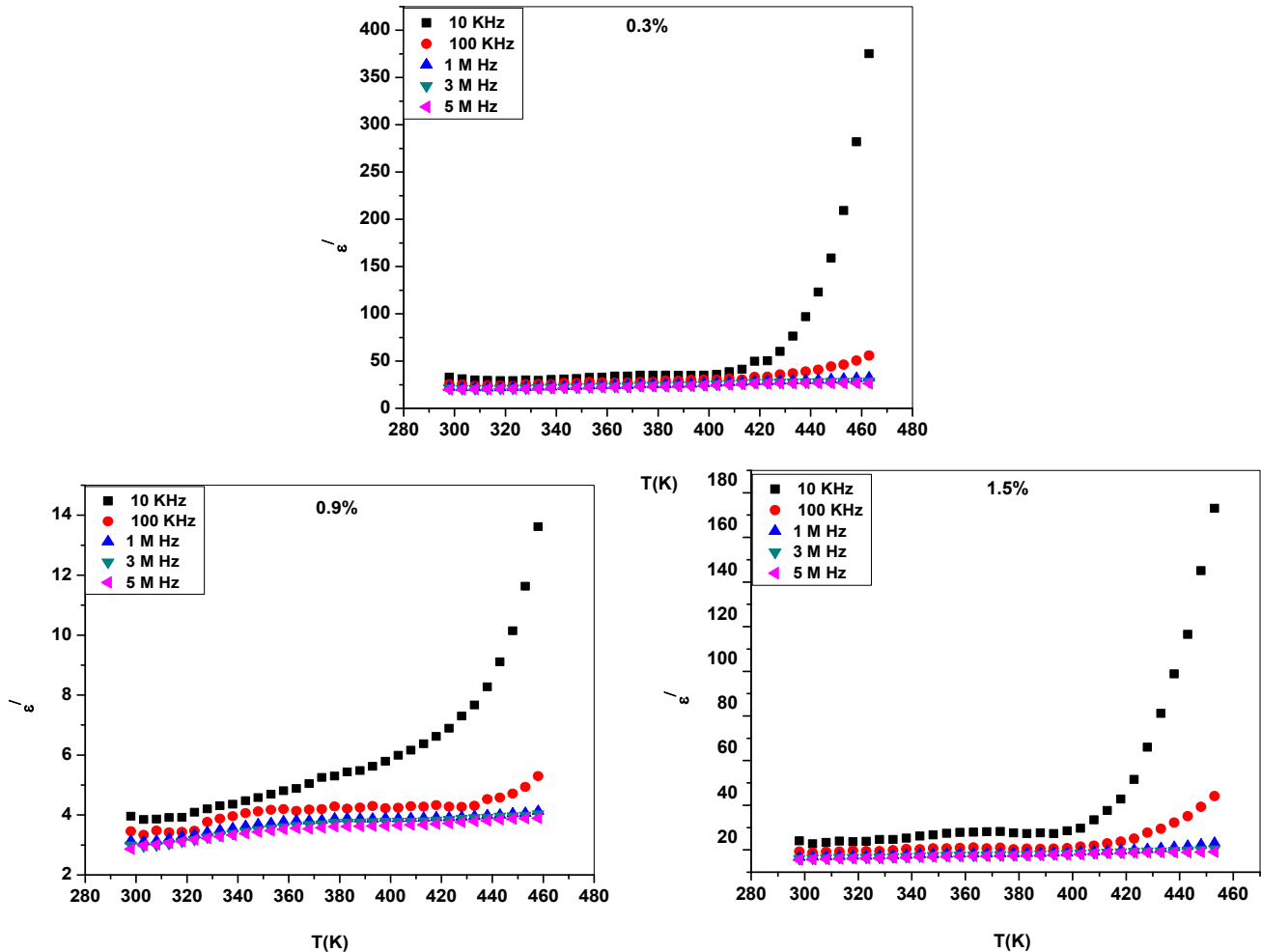


Fig. 5: Dependence of dielectric constant ϵ' , on absolute temperature for of α - Al_2O_3 / PVA/ P(GO) composites in the frequency range 10 kHz- 5 MHz.

hand, at high frequencies, periodic reversal of the electric field occurs so fast that there is no excess ion diffusion in the direction of the field. Polarization due to charge accumulation decreases, leading to the observed decrease in dielectric constant (Reddy et al, 2006).

The obtained values of dielectric constant ϵ' , of P(GO)/ PVA/ α - Al_2O_3 composites at 10 kHz and room temperature shows that, the dielectric constant of the α - Al_2O_3 / PVA matrix is enhanced by the adding P(GO) sheets by its the

MHz. The data at each separate frequency obeys the well known Arrhenius equation:

$$\sigma_{ac} = \sigma_0 \exp(-E/kT)$$

where E is the activation energy, k is the Boltzmann's constant and T is the absolute temperature. The data showed that, the ac conductivity (σ_{ac}) increases with increasing frequency; which acts as a pumping force, pushing the charge carriers between the different conduction states. Also, the

conductivity increases with increasing temperature with changing the slope at a certain temperature which is general trend of

P(GO). A series of P(GO)/PVA/ α -Al₂O₃ hybrid films was prepared by the casting method. XRD, FTIR,. The properties of virgin PVA is modified

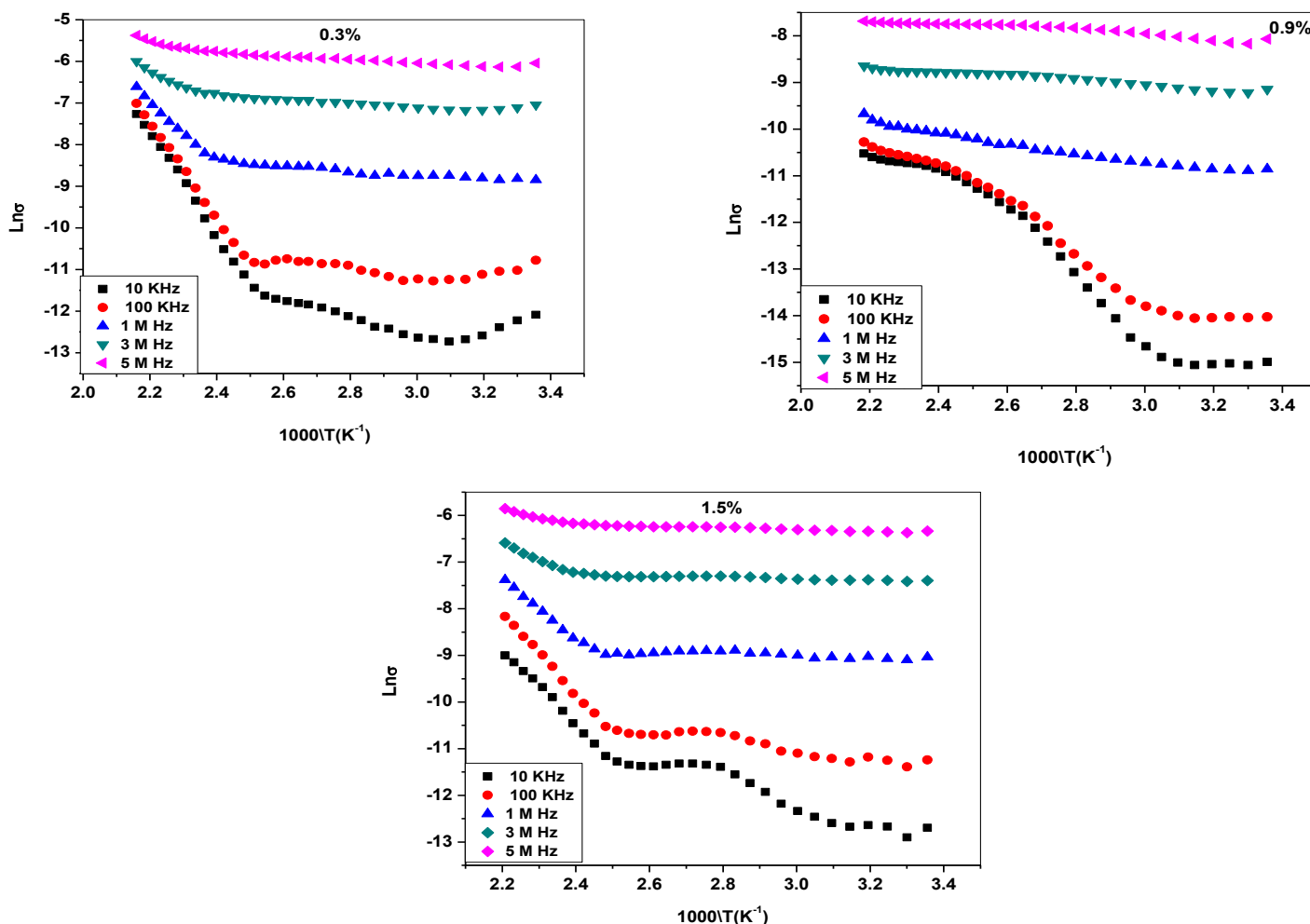


Fig. 6: Dependence of ac conductivity on the reciprocal of the absolute temperature for α -Al₂O₃/PVA/ P(GO) composites in the frequency range 10 kHz- 5 MHz.

semiconductor like behavior. The activation energies values show that all the samples have two regions with changing slope at different temperatures, i.e., the conduction mechanism changes from one region to another region (Ahmed et al, 2013).

4. Conclusion

GO nanoparticles were successfully prepared using Hummers and Offman method. XRD spectrum shows that the prepared sample is

and improved by doping with GO NPs and P(GO) sheets, making it a promising material for different applications.

References:

1. Ueda W., Sadakane M., Ogihara H., Nano-structuring of complex metal oxides for catalytic oxidation,” Catalysis Today, 132, 2008.
2. Gessner T., Gottfried K., Hoffmann R. et al., “Metal oxide gas sensor for high

- temperature application,” *Microsystem Technologies*, 6 2000 (169–174).
3. Kim J. H., Kim E. K., Lee C. H., Song M. S., Kim Y.-H., and Kim, “Electrical properties of metal-oxide semiconductor nano-particle device,” *Physica E*, 26, 432–435, 2005.
 4. Pria P. D., “Evolution and new application of the alumina ceramics in joint replacement,” *European Journal of Orthopaedic Surgery and Traumatology*, 17, no. 3, 253–256, 2007.
 5. Farsi H. and Gobal F., “Theoretical analysis of the performance of a model supercapacitor consisting of metal oxide nanoparticles,” *Journal of Solid State Electrochemistry*, 11, 1085–1092, 2007.
 6. Dillon A. C., Mahan A. H., Deshpande R., Parilla P. A., Jones K. M., and Lee S.-H., “Metal oxide nano-particles for improved electro chromic and lithium-ion battery technologies,” *Thin Solid Films*, 516, 794–797, 2008.
 7. Mallakpour^{1,2} Shadpour and Dinari Mohammad, “Enhancement in thermal properties of poly(vinyl alcohol) nanocomposites reinforced with Al₂O₃ nanoparticles” *Journal of Reinforced Plastics and Composites* 32(4) 217–224, 2013.
 8. Yan D., He J., Li X., Jianxin L., Huili Ding Z., *Surf. Coat. Technol.* 141 (2001) 1.
 9. Chang Y.-S., Roy N., *Vac J. Sci. Tec.* 7 (1989) 1303.
 10. Nahar R. K., Khanna V. K., *Sens. Actuators, Int. J. Electron.* 52 (1982) 557.
 11. Werner F. et al. “Silicon surface passivation by Al₂O₃: Recombination parameters and inversion layer solar cells” *Energy Procedia* 27 (2012) 319–324.
 12. Boratto Miguel Henrique et al. “Hetero junction between Al₂O₃ and SnO₂ Thin Films for Application in Transparent FET” *Materials Research*. 2014; 17(6): 1420-1426.
 13. Thomas S., Recent advances in polymer nanocomposites synthesis and characterisation. 2010; Taylor and Francis Group, LLC.
 14. Mai, Y. W., et al. *Polymer nanocomposites*. 2006; Woodland Publishing.
 15. Sunil K Sahi, PhD, The University of Texas at Arlington, 2016 Copyright © by Sunil Kumar Sahi 2016.
 16. Tantis, Psarras G. C., Tasis D., *Polymer Letters Vol. 6, No. 4* (2012) 283–292.
 17. Morozov, S. V., Novoselov, K. S., Katsnelson, M. I., Schedin, F., Elias, D. C., Jaszczak, J. A., Geim, A. K. Giant Intrinsic Carrier Mobilities in Graphene and Its Bilayer. *Phys. Rev. Lett.* (2008) 100.
 18. Rene H. J. Vervuurt, Bora Karasulu, Marcel A. Verheijen, Wilhelmus (Erwin) M. M. Kessels, and Ageeth A. Bol, “Uniform Atomic Layer Deposition of Al₂O₃ on Graphene by Reversible Hydrogen Plasma Functionalization” *Chem. Mater.* 29 (2017) 2090–2100.
 19. Ghosh D., Lim J., Narayan R., and Sang O. K., *ACS Appl. Mat. Interfaces* 8 (2016) 22253.
 20. Liu S., Yao F., Oderinde O., Zhang Z., and Fu G., *Carbohydr. Polym.* 174 (2017) 392.
 21. Xiang C., Guo R., Lan J., Jiang S., Wang C., Du Z., and Cheng C., *J. Alloys Compd.* 735, 246 (2018).
 22. Dervin S., Lang Y., Perova T., Hinde S. H. r, and Pillai S. C., *J Non-Cryst Solids* 465 (2017) 31.
 23. Ren Lili, and He He, “Effect of the addition of graphite oxide on the morphology of the alumina aerogels” *AIP Advances* 8, (2018) 015208.
 24. Hummers WS, Offeman RE: Preparation of graphitic oxide. *J Am Chem Soc*, 1958, 80(6):1339.
 25. Huang Yiwan, Zeng Ming, Ren Jie, Wang Jing, Fan Liren, Xu Qingyu, *Colloids and Surfaces A: Physicochem.*, 401 (2012) 97–106.
 26. Saravanakumar Balasubramaniam, Mohan Rajneesh, Sang-Jae Kim,

- Materials Research Bulletin 48 (2013) 878–883.
27. Shahriary Leila, Anjali A. Athawale, International Journal of Renewable Energy and Environmental Engineering, 02 (2014) 58- 63
 28. Wu Nan, She Xilin, Yang Dongjiang, Wu Xiaofeng , Su Fabing , Chen Yunfa, Chem., J. Mater. 22 (2012) 17254-17261.
 29. Si Y., and Samulsk E. T. i, Nano Lett. 8 (2008) 1679- 1682.
 30. Jothi Ramalingam K., Dhineshababu N.R., Srither S.R., Saravanakumar B., Synthetic Metals, 191 (2014) 113-119.
 31. Xu Y., Bai H., Lu G., Li C., Shi G., Am J. Chem. Soc. 130 (2008) 5856- 5857.
 32. Chen Chen, Long Migce, Xia Min, Zhang Chunhua, Cai Weimin, Nanoscale Research Letters, 7 (2012) 101-105.
 33. Zhang Henan, Hines Deon, Akins Daniel L., Dalton transactions, 43 (2014) 2670-2675.
 34. Yuan X., Polym. Bull. 67 (2011) 1785–1797.
 35. Roy Aashis S., Gupta Satyajit, Sidhu S., Ameena Parveen, Ramamurthy Praveen C., Composites, 47 (2013) 314-319.
 36. Gunassekaran S, Sailatha E, Sesshadri S, Kumaresan S, Indian Journal of Pure and Applied Physics, 47 (2009) 12- 18.
 37. Keskin Selda, Ibrahim Uslu, Tunc Tuncay, Öztür Mustafa, Arda Aytimur, Mater. Manuf. Processes 26 (2011) 1346- 1351.
 38. Ali Z., Youssef H., Afify T., Polym. Comp., 105 (2007) 2976- 2980.
 39. Hemalatha K.S., Rukmani K., Suriyamurthy N., Nagabhushana B.M., Materials Research Bulletin 51 (2014) 438–446. Dielectric properties.
 40. Ng B. C., Wong H. Y., Chew K. W., Z. Osman, International Journal of Electrochemical Science 6 (2011) 4355–4364.
 41. Reddy C. V. S., X., Han Zhu Q., Mai L., Chen W., Microelectronic Engineering, 83 (2006) 281–285.
 42. Ahmed M.A., Mansour S.F., Abdo M.A., Materials Research Bulletin, 48 (2013) 1796–1805.